

**INFLATION FEATURES ON THE DISTAL PAHOEHOE PORTION OF THE 1859 MAUNA LOA FLOW, HAWAII: IMPLICATIONS FOR EVALUATING PLANETARY LAVA FLOWS.** J. R. Zimbelman<sup>1</sup>, W. B. Garry<sup>1,2</sup>, J. E. Bleacher<sup>3</sup>, and L. S. Crumpler<sup>4</sup>, <sup>1</sup>CEPS/NASM MRC 315, Smithsonian Institution, Washington, D.C. 20013-7012, zimbelmanj@si.edu; <sup>2</sup>Planetary Science Institute, Tucson, AZ; <sup>3</sup>Planetary Geodynamics Laboratory, Code 698, NASA Goddard Space Flight Center, Greenbelt, MD 20771; <sup>4</sup>New Mexico Museum of Natural History and Science, 1801 Mountain Road NW, Albuquerque, NM 87104.

**Introduction:** The 1859 eruption of Mauna Loa, Hawaii, resulted in the longest subaerial lava flow on the Big Island. Detailed descriptions were made of the eruption both from ships and following hikes by groups of observers [1, 2]; the first three weeks of the eruption produced an ‘a‘ā flow that reached the ocean, and the following 10 months produced a pāhoehoe flow that also eventually reached the ocean [3]. The distal portion of the 1859 pāhoehoe flow component (Figure 1)

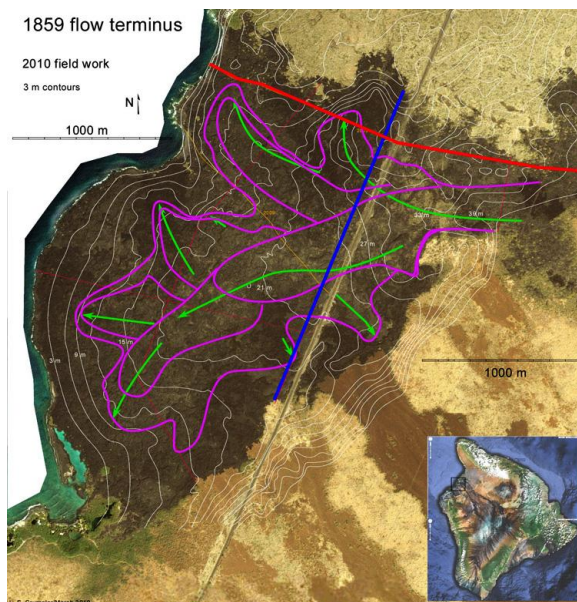


Figure 1. Map of the distal pāhoehoe component of the 1859 Mauna Loa flow. Contours are derived from topography shown in USGS 1:24K maps. Image base is mosaiced air photos from Google Earth. Green lines show local flow directions inferred from both field observations and the regional topography. Purple lines identify discrete flow lobes recognized in the field. . 3. Map produced by LSC. Red line shows location of DGPS data in Fig. 2. Blue line shows location of DGPS data in Fig 3.

includes many distinctive features indicative of flow inflation [4, 5]. Field work was conducted on the distal 1859 pāhoehoe flow during 2/09 and 3/10, which allowed us to document several inflation features, in order evaluate how well inflated landforms might be detected in remote sensing data of lava flows on other planets.

**Observations:** Several inflation features were observed on the 1859 pāhoehoe flow; here we focus on features having the greatest likelihood of being observable on planetary lava flows. Differential Global Positioning System (DGPS) measurements were collected using a Trimble R8 DGPS system, which provides  $\pm 2$  cm horizontal and  $\pm 4$  cm vertical precision [6]. Figure 2 shows a DGPS profile that follows the northern edge

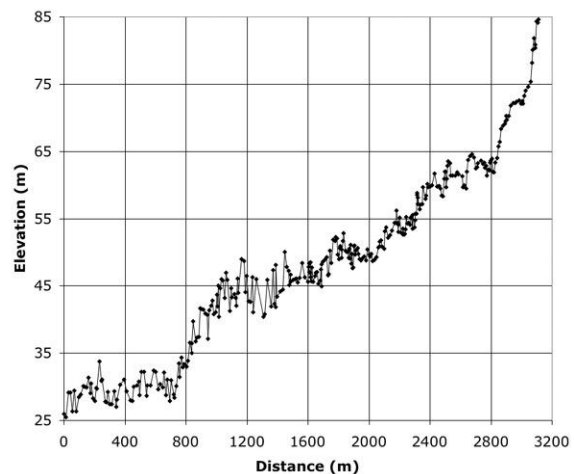


Figure 2. DGPS profile following the flow from the coastline (0 distance) going east to where the flow is on a slope typical of shield volcanoes.

of the flow field (red line, Fig. 1); slopes on the flow surface decrease from typical shield flank values ( $4.5^\circ$ ,  $>3$  km from the coast) to shallow slopes where the inflation features are best expressed ( $0.7^\circ$ , 700 to 2800 m distance in Fig. 2), to a coastal plain ( $0.15^\circ$ , 0 to 700 m distance in Fig. 2). Figure 3 shows a DGPS profile

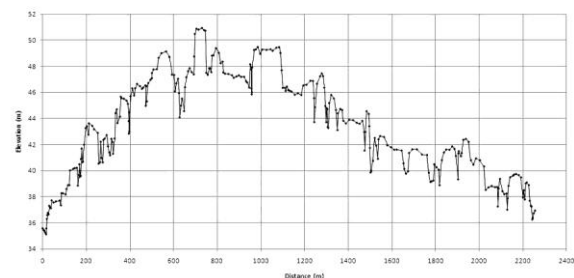


Figure 3. DGPS profile paralleling highway 11, going north to south, across the pāhoehoe flow ‘delta’. Several individual inflated flow lobes are evident.

across the width of the flow field immediately west of state highway 11 (blue line, Fig. 1).

**Lava rise pits.** Walker [4] coined the term ‘lava rise pit’ to distinguish between depressions on lava flows produced by collapse into an evacuated cavity (collapse pit) and depressions resulting from the inflation of a lava flow around an area that experienced little to no inflation (Figure 4a). Distinctive ‘squeeze-outs’ of spiny, striated lava are evident in the walls of many lava rise pits, although such features will be extremely difficult to detect in remote sensing data.

**Inflation plateaus.** When a lava flow lobe becomes inflated, it tends to produce an upper surface with surprisingly uniform topography (see Fig. 3). The level upper surface is surrounded by steep margins where solidified crust was elevated by the flow inflation, resulting in steep margin slopes that can approach becoming vertical (Figure 4b). The top of the margin often has long fractures, 1-2 m wide and generally 3 to 6 m deep; these large margin fractures are readily detectable in m-resolution images [e.g., 7].

**Surface swales.** The tops of some inflation plateaus displayed a distinct ‘swale’ pattern (Figure 4c), where slightly convex pāhoehoe plates (generally 1 – 3 m in width) are present between fractures extending over tens of meters. A similar swale texture is present on the surface of some lava flows on Mars interpreted to be inflated [8], as imaged by the HiRISE camera. The precise mechanism of the swale plate formation remains unclear, but the swale pattern itself might provide supplementary support for the remote identification of inflated flows on other planets.

**Other features.** Tumuli are common on inflated portions of the 1859 pāhoehoe flow, ranging in scale from tens to hundreds of meters in length and generally 3 to 5 m of relief. However, tumuli can also be associated with concentrated internal flow paths within a flow field (as evidenced by aligned tumuli ridges in portions of the Carrizozo flow field, New Mexico [9]), so that the presence of tumuli alone should not be considered sufficient evidence of flow inflation.

**Conclusions:** Field examination of inflation features on the distal pāhoehoe portion of the 1859 Mauna Loa flow revealed certain characteristics that can be considered indicative of flow inflation, but many such features will be very difficult to detect in typical remote sensing data. The level tops of inflation plateaus, some possibly displaying a distinctive swale texture, may be one good remotely determined indicator that inflation has taken place.

**Acknowledgements:** This work was supported by a Scholarly Studies grant from the Smithsonian Institution, which is complimentary to the science objectives of NASA PGG grant NNX09AD88G.

**References:** [1] Barnard W. M. (Ed.) (1990) Mauna Loa – A Source Book. SUNY College Fredonia, Fredonia, NY. [2] Barnard W. M. (1991) In Mauna Loa Revealed (J.M. Rhodes and J. P. Lockwood, Eds.), AGU Monogr 92, 1-20. [3] Rowland S. K. and Walker G. P. L. (1990) Bull. Volc. 52, 615-628. [4] Walker G. P. L. (1991) Bull. Volc. 53, 546-558. [5] Walker G. P. L. (2009) In Studies in Volcanology (T. Thordarson et al., Eds.), IAVCEI Sp Pub 2, Geol. Soc. London, 17-32. [6] Zimbelman J. R. and Johnston A. K. (2001) In Volcanology in New Mexico (L. S. Crumpler and S. G. Lucas, Eds.), NMMNHIS Bull. 18, 131-136. [7] Garry W. B. et al. (2011) LPS XXXXII (this volume). [8] Zimbelman J. R. et al. (2010) LPS XXXXI, Abs #1826. [9] Zimbelman J. R. and Johnston A. K. (2002) NM Geol. Soc. Guidebook, 53<sup>rd</sup> Field Conf., 121-127.



Figure 4. Field views of typical inflation features on the 1859 pāhoehoe flow. a) Lava rise pit, ~20 m in diameter. b) Margin of an inflation plateau. Note person for scale. c) Swales on the upper surface of an inflation plateau. All photos, JRZ, 2/09.